JOURNAL OF THERMOPHYSICS AND HEAT TRANSFER
Vol. 11, No. 2, April–June 1977

Effect of H_2O Vapor on the Vibrational Relaxation in Hypersonic Wind Tunnels

Véronique Joly* and Claude Marmignon†
ONERA, 92322 Châtillon, France

This study concerns the development of numerical methods for the simulation of flows in thermochemical nonequilibrium. Its purpose is to take into account some additional minor chemical species in the Navier–Stokes solver CELHYO developed at ONERA. To solve the problem the time-dependent set of equations that governs the flow of the major constituents (N_2, O_2, NO, N, O) and of the contaminants is used. The method is applied to the effect of a contaminant such as H_2O vapor on the vibrational relaxation of N_2 and O_2 in two different hyperenthalpic wind tunnels: 1) the ONERA F4 hyperenthalpic wind tunnel and 2) the LBK of the DLR. The modifications of important flow parameters such as the temperatures and the Mach number at the nozzle exits are presented.

I. Introduction

IN the frame of the research on atmospheric re-entry vehicles, hypersonic ground-testing facilities such as the ONERA F4 wind tunnel are necessary for understanding hyperenthalpic flows of air. They provide data more easily and cheaper than flight tests. However, the chemical composition of flows in these facilities is specific to each wind tunnel and more complex than air.[1] Indeed, the temperature reached in the chamber is so high that the flow is highly dissociated and may also contain unwanted chemical species coming from, for example, the vaporization of the electrodes or the chamber lining during the run. Water may also be present in small amounts with a mass fraction of the order of 0.001 in the F4 wind tunnel, as a combustion product of the chamber, or in greater abundance, reaching perhaps a mass fraction of the order of 0.02 or more in the LBK wind tunnel, as a component of the atmospheric air used in the facility. These water mass fraction values are estimations that have to be experimentally measured for confirmation. Thus, to compare experimental results with numerical ones and to precisely validate the nonequilibrium computational solvers, a chemistry model as realistic as possible has to be implemented in the solver. This requires additional chemical species different from the usual five species N_2, O_2, NO, N, and O to be considered, and all of the significant chemical processes existing between these species and the major constituents in the wind tunnel are to be taken into account. The validated solvers could then be reliably used to accurately predict the flow in the flight conditions.

In this study we will focus our attention on the chemical species that vibrationally relax the molecules N_2 and O_2 during the expansion, according to the important energy transfer processes within internal degrees of freedom. We will consider the very active water-vapor catalyst for which reaction rates are available.

II. Background

Our interest in minor components started after an experimental coherent anti-Stokes Raman scattering (CARS) campaign carried out by an ONERA group at the LBK wind tunnel of DLR.[2] The pressure and temperature reservoir conditions were, respectively, $p_0 = 1.29 \times 10^5$ Pa and $T_0 = 3748$ K. The total density and the rotational temperature of N_2 in the freestream flow were measured at the nozzle exit. A maximum for the vibrational temperature of N_2 was also determined at this location. These measurements were obtained by recording rotationally resolved spectra of the different vibrational bands in a probe volume where the CARS beams were focused. As is customary in CARS,[3] information about the state of the molecular system was derived from line shapes and line intensities. Then, numerical simulations of the flow were performed with the CELHYO code[4] (see next paragraph for more details about this solver) without taking impurities into account. Concerning the density and the translational temperature (assuming as usual $T_{\rm rot} = T_{\rm trans}$), the comparison of experimental results with the numerical results was satisfactory. However, the calculated N_2 vibrational temperature was found to be much greater than measured.

The fact that N_2 relaxes much faster in an expansion is an old problem that has been described by many authors, but the reasons explaining this behavior are still controversial. For example, Hurle et al.[5] inferred from measurements in supersonic nozzle flows of N_2 that the probability of N_2 vibrational de-excitation was about 15 times greater than that inferred from measurements of vibrational relaxation made behind normal shock waves. Tentative reasons such as the applicability of the Landau–Teller relaxation equation and the possibility of alternative and more rapid mechanisms were considered as possible explanations for the observed relaxation, but it was not clear at that time if either of these reasons were correct.

To account for the CARS campaign results, we were first interested in the copper species, as an impurity coming from the chamber during the operation of the LBK wind tunnel. From the mass loss of the electrodes, the Cu mass fraction in the gaseous mixture was found to be less than 10^{-4}, which appeared to be small. But the vibrational de-excitation of N_2 by collisions with Cu could perhaps be significant. The reaction rates for the N_2 vibrational relaxation by metal atoms (Li, Na, K, Cs, and Al) have been estimated,[6] and these rates are very large, sometimes close to the gas kinetic collision rate (each collision being efficient). This might also be the case for Cu because, like some of these atoms, Cu has an unpaired electron that seems responsible for these large rates.[7] Unfortunately, no data are now available for this species.

The LBK wind tunnel was operated during this experiment using atmospheric air. Some water vapor was present in the flow, its mass fraction being not measured. Considering that

---

Presented as Paper 96-1855 at the AIAA 31st Thermophysics Conference, New Orleans, LA, June 17–20, 1996; received July 20, 1996; revision received Dec. 1, 1996; accepted for publication Dec. 12, 1996.

*Research Engineer, Theoretical Aerodynamics Branch 1, B.P. 72. E-mail: joly@onera.fr.

†Research Engineer, Theoretical Aerodynamics Branch 1, B.P. 72. E-mail: marmigno@onera.fr.

the air humidity might contribute to a maximum water mass fraction equal to 1.6×10^{-2} (corresponding to maximum humidity according to the saturating vapor pressure), and considering also that potential microleaks might exist in the cooling system, a value equal to 2×10^{-2} for the water mass fraction was inferred. This value was found to enable sensitive calculations with respect to the effect of water vapor in the flow. H_2O is known to catalyze the vibrational relaxation of numerous molecules. For example, its effect on the vibrational relaxation of N_2 ($v = 1$) is several orders of magnitude more efficient than that of other N_2 molecules. This stems from the ability of H_2O to create strong attractive forces with its collision partners and from the efficiency of its rotational motion in removing the transferred vibrational energy.[8,9]

In an attempt at taking into account in the CELHYO code the effect of some gaseous de-exciting species, a bibliographic search was carried out to know the temperature dependences of the relaxation reaction rates of N_2 and O_2 by H_2O (with data banks CEDOCAR, NTIS, Chemical Abstracts at ONERA, and GAPHYOR at the University of Paris). The intrinsic physical data of H_2O were also collected. The search also covered Cu as a catalyst, but no information was obtained for this species. The results are given in Sec. IV.C.

III. CELHYO Solver

The Navier–Stokes code CELHYO[4] for hypersonic laminar viscous flows in chemical and thermal nonequilibrium was developed at ONERA. With this code, one- and two-dimensional high-enthalpy flows can be simulated.

A. Basic Assumptions

The CELHYO code treats mixtures of perfect gases made of n_h heavy species, n_m of them being molecular species. The mixture is usually assumed to be made of the five neutral species N_2, O_2, NO, N, and O, but may also contain some contaminants. All of the species are described with the same mean velocity v. Three degrees of freedom are considered: 1) translation and rotation, described by one temperature T_{trans}; 2) vibration; and 3) dissociation. Energy is supposed to follow a Boltzmann distribution. We assume that n_v molecular species, $1 \leq n_v \leq n_m$, have their own vibrational temperature T_{vj}, $j \in [1, \ldots, n_v]$, such as N_2 and O_2 for air. For contaminants such as H_2O, which relaxes very quickly (see next paragraph), and Cu which is an atom, no supplementary vibrational temperature is needed. However, CO_2, for example, could not be considered to be at equilibrium: it is usual to consider two vibrational modes.[10] The second-order diffusive convective system governing the mixture under consideration writes

$$\partial_t u + \mathrm{div}[f(u) - D(u)\mathrm{grad}u] = \Omega \tag{1}$$

where f denotes the inviscid fluxes. Dissipative phenomena are modeled by the diffusive tensor D. The source term Ω represents the presence of nonequilibrium phenomena. The variable u is

$$u^T = [(\boldsymbol{\rho}_\alpha)_{1\leq\alpha\leq n_h}, \boldsymbol{\rho} v_1, \rho v_2, \rho E, (\rho_{\boldsymbol{\beta}} e_{v\beta})_{1\leq\beta\leq n_v}] \tag{2}$$

where E denotes total energy of the mixture and $v = (v_1, v_2)$ is the mean velocity. $e_{v\beta}$ refers to the vibrational energy of the molecular species $\boldsymbol{\beta}$ assumed to be in thermal nonequilibrium. The mixture pressure p is defined by

$$p = \kappa_{\mathrm{tr}} \left\{ \rho E - \frac{1}{2}\rho v^2 - \sum_\beta \rho_\beta e_{v\beta} - \sum_\alpha \rho_\alpha [h^0_\alpha + e_\alpha(T)] \right\} \tag{3}$$

where $\kappa_{\mathrm{tr}} = \gamma_{\mathrm{tr}} - 1$. e_α and h^0_α, respectively, refer to the energy of the internal modes at equilibrium with translation and the heat of formation of species α.

Detailed expressions of source terms and the diffusive tensor may be found in a previous paper.[4] The chemical reaction model taken for air is Gardiner's.[11] It consists of 15 dissociation reactions and two exchange reactions. The vibrational relaxation of diatomic species (N_2 and O_2 for air) occurs through V–T transfers that are modeled following the Landau–Teller rule,[12] and using the data given in Ref. 13 for the collisions with molecules (N_2, O_2, and NO) and in Ref. 14 for the collisions with atoms (N and O). V–V processes can also be taken into account with the formulation for the source term and the data given in Ref. 14. For the collisions of N_2 or O_2 with H_2O, the data are given in the next paragraph. A no-slip condition together with a constant temperature for the translational and vibrational modes are prescribed at the wall boundary. The wall can be assumed to be either fully catalytic or noncatalytic.

B. Numerical Method

The CELHYO code solves the Navier–Stokes balance equations on curvilinear structured meshes using a fully implicit, finite volume method. The viscous part is discretized according to a central-differencing procedure, whereas a quasi-second-order-accurate upwind scheme yields an approximation for the inviscid operator. Upstreaming is achieved using an approach for upwind bias referred to as the hybrid upwind splitting.[15] The method is designed to combine the natural strengths of the Osher solver and the Van Leer splitting to get accuracy in the resolution of boundary layers and robustness in the capture of nonlinear waves, respectively. It is emphasized that no switch to be tuned up is involved here. Second-order accuracy is achieved using a MUSCL approach written in primitive variables. Special attention is paid when the method is applied to mass fractions to preserve the local number of elements.

The implicit operator is made up of a linearization of both the inviscid and viscous fluxes plus all of the source term Jacobian matrices. For a detailed presentation of this time-marching algorithm, the reader is referred to Ref. 4.

IV. Energy Transfer Processes

For a better understanding of the mechanisms occurring during N_2 (or O_2)-H_2O collisions, we recall some general results about V–T, R and V–V couplings.[16]

A. Background

Let us consider a vibrationally excited molecule A^*. For example, the asterisk may denote one quantum of vibrational excitation. A^* collides with a species M and the vibrational energy is transferred into translational motion. This process may be expressed kinetically as

$$A^* + M \overset{k_f}{\underset{k_r}{\rightleftharpoons}} A + M \tag{4}$$

where A represents the molecule in its ground state. This is called a vibration–translation or V–T process (or coupling). As the vibrational energy can go directly into translational motion or into rotation of the collision partners and then into translational motion, V–T processes are sometimes written V–R, T. k_f and k_r are the forward and reverse reaction rates, respectively, generally expressed in $\mathrm{cm}^3\,(\mathrm{mol}\cdot\mathrm{s})^{-1}$, or even in $(\mathrm{atm}\cdot\mathrm{s})^{-1}$. [$k\ \mathrm{cm}^3\,(\mathrm{mol}\cdot\mathrm{s})^{-1} = 10^6(P_{\mathrm{atm}}/P_{\mathrm{Pa}})k_B T\,(\mathrm{K})\ k\,(\mathrm{atm}\cdot\mathrm{s})^{-1}$, where P_{atm} and P_{Pa} are, respectively, the pressure expressed in atmosphere and in Pascal, and k_B is the Boltzmann constant.]

Usually, the larger the vibrational quantum, the slower the rate for that process. This is because of the poor coupling between the fast vibrational motion and the slower translational motion leading to an adiabatic collision with small or no energy transfer. Hence, only the high-velocity tail of the Boltzmann distribution is effective in most V–T transfer processes. Obviously, transfer rates increase with temperature.

Such processes generally show a very steep temperature dependence

$$k \propto \exp[-(1/T^{1/3})]$$

Vibrational energy can also be exchanged between the vibrational modes of two molecules:

$$A^* + B \underset{k_r'}{\overset{k_f'}{\rightleftharpoons}} A + B^* \qquad (5)$$

This is called a vibration–vibration (V–V) process. V–V processes have generally much larger rate constants than V–T reactions. Energy resonant or near-resonant V–V processes are among the fastest of vibrational energy transfer reactions. Also, for V–V processes an inverse or slightly positive temperature dependence is usual

$$k' \propto \exp[\pm(1/T)]$$

For many kinetic applications, the rate-determining step is the most important process. Since relaxation through a V–V energy transfer is often much faster than relaxation through a V–T channel during cascades, V–V exchanges should not be neglected. However, there are always some exceptions to the previous statement. For example, when M is an atom or a radical, fast rates are generally observed for the V–T process, although the details of the molecular interaction are not precisely understood. Concerning H_2O, the relaxation of O_2 or N_2 by collisions with this species exhibit a particular behavior, as is shown in Sec. IV.B.

B. Tuesday and Boudart Theory

The N_2–H_2O and O_2–H_2O systems are two examples of a system written A–H_2O, in which both components are excitable. Following the theory of Tuesday and Boudart,[17] the deexcitation of the vibrational degrees of freedom takes place by means of five processes ($A = N_2$ or O_2):

$$A^* + X \underset{k_{01}}{\overset{k_{10}}{\rightleftharpoons}} A + X \qquad (6)$$

$$A^* + H_2O \underset{k_{02}}{\overset{k_{20}}{\rightleftharpoons}} A + H_2O \qquad (7)$$

$$A^* + H_2O \underset{k_{03}}{\overset{k_{30}}{\rightleftharpoons}} A + H_2O^* \qquad (8)$$

$$H_2O^* + H_2O \underset{k_{04}}{\overset{k_{40}}{\rightleftharpoons}} H_2O + H_2O \qquad (9)$$

$$H_2O^* + X \underset{k_{05}}{\overset{k_{50}}{\rightleftharpoons}} H_2O + X \qquad (10)$$

The excited species A^* is, respectively, N_2 ($v = 1$) or O_2 ($v = 1$), the most populated excited levels. X denotes the collisional partners other than H_2O, which are N_2, O_2, NO, N, and O in this study. The mechanisms (7–10) are the result of the presence of water in the flow and are to be considered in addition to process (6). Process (6) summarizes the different mechanisms of the vibrational relaxation of N_2 and O_2 during collisions with the molecules (N_2, O_2, and NO) and the atoms (N and O), mechanisms that are taken into account in the CELHYO code (cf., Sec. III.A) and are not detailed here. The vibrational energy-level diagram for the N_2–H_2O and O_2–H_2O molecular systems is given in Fig. 1. The H_2O molecule is nonlinear and has three fundamental frequencies corresponding to the symmetric (ν_1), deformation (ν_2), and asymmetric (ν_3) types of vibration. The H_2O vibrational relaxation by collisions with other molecules or atoms has been the subject of many experimental and theoretical works.[8,18–20] For the present study, the excited species H_2O^* corresponds to the first vibrationally excited level H_2O (ν_2, $v = 1$).

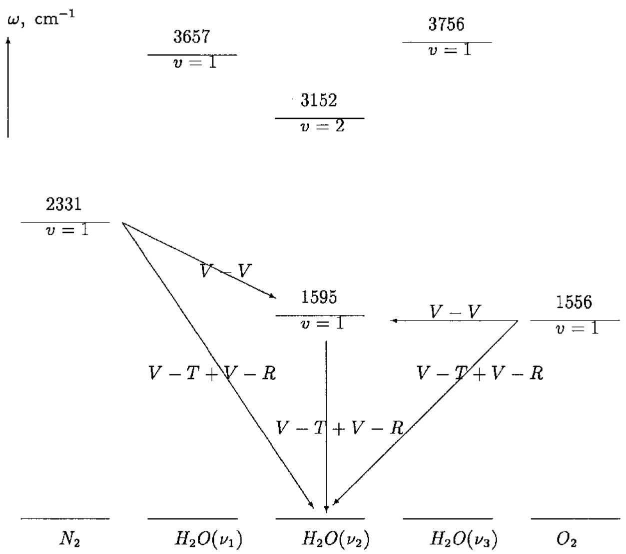

Fig. 1 Vibrational energy diagram.

Processes (6), (7), (9), and (10) represent a V–T, R coupling [processes (6) with $X = A$ and (9) are self-relaxation reactions], whereas process (8) is a V–V coupling. [In fact, for process (9), an additional dominant V–V transfer of vibrational energy through the oscillatory motion of weakly bound complexes has to be considered at $T < 1000$ K[8,20]]. Process (9) is extremely rapid for all of the temperatures, its reaction rate being close to the gas kinetic collision rate [$k_{gk} = 2 \times 10^{-10}$ cm^3 (mol·s)$^{-1}$ at 300 K]. Process (10) is very rapid also [about 3×10^{-13} cm^3 (mol·s)$^{-1}$ at 300 K and about 3×10^{-12} cm^3 (mol·s)$^{-1}$ at 2000 K for $X = N_2$ or O_2]. For these reasons, we assumed in our calculations the $H_2O(\nu_2)$ mode to be at equilibrium with the translational temperature. We have also assumed that the three vibrational temperatures of H_2O corresponding to the three modes are equal.

Process (8) may be important because it is not limited by processes (9) or (10), as in the case of a usual V–R, T coupling. We may have to consider the V–V energy transfers for the N_2–H_2O and O_2–H_2O systems.

Process (6) for $A = N_2$ or O_2 and $X = N_2$ or O_2 is slow compared to process (7) (see Sec. IV.C for numerical values). Processes (7) and (8) are the V–R, T and V–V couplings for which our bibliographical research has provided the reaction rates as a function of the temperature.

C. Bibliographical Research Results

1. N_2–H_2O

The vibrational relaxation of N_2 by H_2O has been the subject of many articles. Acoustic measurements,[21] shock-tube experiments,[9,22–24] and calculations[9,25–27] have been carried out in the temperature range of 300–3000 K.

As can be seen in Fig. 1, process (8) for N_2 is not close to resonance (800 cm^{-1} difference) and processes (9) and (10) are not limiting steps. Thus, it is difficult in this case to separate the V–R, T and V–V contributions. Concerning the experimental studies, authors generally interpret their data in terms of a V–T coupling only, like Rosenberg et al.[23] and Center and Newton.[24] Zuckerwar and Meredith[21] use a V–V interpretation. Taylor and Bitterman[22] give separately the two interpretations (V–T only or V–V only). Kurian and Sreekanth[9]

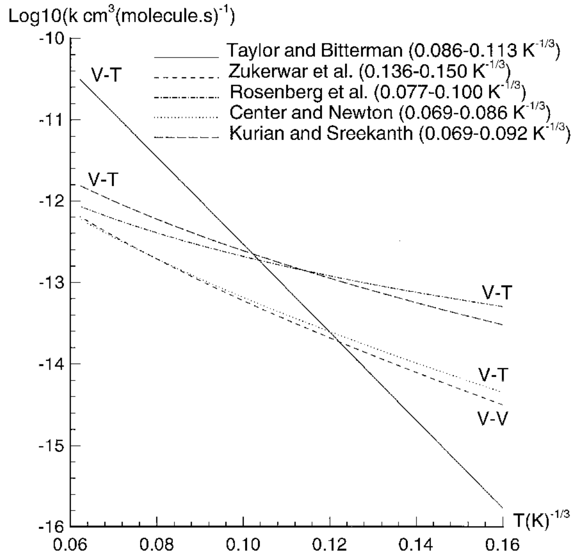

Fig. 2 Vibrational relaxation of N_2 by H_2O (experimental studies).

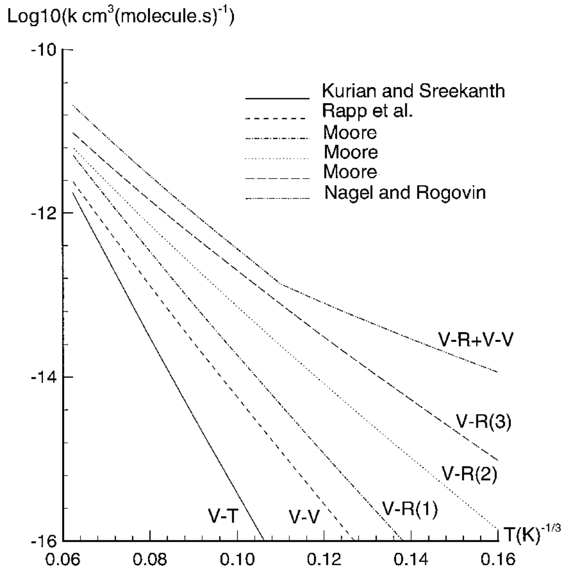

Fig. 3 Vibrational relaxation of N_2 by H_2O (calculations).

describe a method that allows one to take into account both mechanisms. Unfortunately, they cannot apply it to their measurements because of a lack of data points at each temperature. Then they only deduce *V–T* rates. The experimental laws are drawn in Fig. 2 as a function of T (K)$^{-1/3}$ varying from 0.06 to 0.16 K$^{-1/3}$ and the ranges where the experimental results have been obtained are specified.

These various interpretations do not lead to difficulties if each vibrational relaxation time remains associated with the process that has been chosen for its determination. However, the data supplied by the various authors are not in good agreement, which shows the difficulty to infer precisely such rates. For the calculations with the CELHYO code, a low *V–T* reaction rate $k_C^{N_2}$ cm^3 (mol·s)$^{-1}$ (Ref. 24) and a rapid *V–T* one k_B^{N2} cm^3 (mol·s)$^{-1}$ (Ref. 22) (see Fig. 2) have been tested:

$$k_C^{N_2} = 5.32 \times 10^{-16} T \text{ (K)} \exp[-(21/T^{1/3})] \tag{11}$$

$$k_{TB}^{N_2} = 7.1 \times 10^{-08} \exp[-(124/T^{1/3})] \tag{12}$$

The theoretical determinations are, in the same way, based on different assumptions: Kurian and Sreekanth[9] estimate first the *V–T* relaxation rate by using the Schwartz, Slawsky, and Herzfeld theory.[28] In fact, this theory is not well adapted for polar rotors such as H_2O. Then they also consider a *V–V* coupling, following Rapp's theory given in Ref. 25. But the temperature dependence is too steep. Moore[26] proposes three *V–R* models corresponding to the adjustment of specific interaction parameters that are adapted by Kurian and Sreekanth[9] to the N_2–H_2O system. Nagel and Rogovin[27] consider the two processes (*V–V* + dominant *V–R*) with a change of slope at $T = 750$ K. These theoretical determinations (also scattered) are shown in Fig. 3.

Some orders of magnitude of the reaction rates of the N_2 vibrational relaxation are here given for comparison: at 1500 K, the reaction rate is 10^{-13} to 10^{-12} cm^3 (mol·s)$^{-1}$ for N_2–H_2O (*V–T*), whereas it is about 10^{-17} cm^3 (mol·s)$^{-1}$ for N_2–N_2 (*V–T*) and 10^{-14} cm^3 (mol·s)$^{-1}$ for N_2–O (*V–T*).[14] Note that the relaxation by collisions with atomic oxygen is fast, according to our previous remark.

2. O_2–H_2O

The O_2 vibrational relaxation by H_2O has been studied less in comparison with the N_2–H_2O system. Some acoustic measurements[29] are available. They give an order of magnitude for processes *V–T* and *V–V* that are observed. In this case, the *V–V* coupling is quasiresonant and processes (9) and (10) are not limiting steps. Thus, *V–T* and *V–V* processes are well separated, the *V–V* process being much more rapid at ambient temperature than the *V–T* one. Following Bass et al.,[29] at 300 K, the reaction rate is about 10^{-14} to 10^{-13} cm^3 (mol·s)$^{-1}$ for the *V–T* coupling, 10^{-12} to 10^{-11} cm^3 (mol·s)$^{-1}$ for the *V–V* coupling, compared to 10^{-18} cm^3 (mol·s)$^{-1}$ for the O_2–O_2 *V–T* coupling and 10^{-12} cm^3 (mol·s)$^{-1}$ at 1000 K for O_2–O (*V–T*) (Ref. 14) (fast relaxation).

We have only found two laws for the dependence of the *V–T* reaction rate with the temperature. One is given by Taylor,[16] in the range of 200–5000 K, as a maximum value

$$k_T^{O_2} < 3.6 \times 10^{-10} \exp[-(60.69/T^{1/3})] \text{ cm}^3 \text{ (mol·s)}^{-1} \tag{13}$$

The other one comes from the compilation of Blauer and Nickerson[30] and Nickerson[31] in the range of 400–1600 K

$$k_{BN}^{O_2} = 5.3 \times 10^{-6} \exp[-(124/T^{1/3})] \text{ cm}^3 \text{ (mol·s)}^{-1} \tag{14}$$

At $T = 300$ K, these two laws give the same result, about 4×10^{-14} cm^3 (mol·s)$^{-1}$. But the difference reaches two orders of magnitude at 1500 K [about 1.8×10^{-12} cm^3 (mol·s)$^{-1}$ and 10^{-10} cm^3 (mol·s)$^{-1}$]. Again, the scattering in the results seems important.

For the *V–V* coupling, Lang[32] made a compilation of acoustic measurements in the range of 300–800 K, which yields

$$k_L^{O_2} = 2.9 \times 10^{-12} \exp[-(55.8/T)] \text{ cm}^3 \text{ (mol·s)}^{-1} \tag{15}$$

At 300 K, the reaction rate is about 2×10^{-12} cm^3 (mol·s)$^{-1}$. This process will be important to consider, especially at low temperature.

V. Applications

A. F4 Wind Tunnel

To compare the models presented in the previous paragraph, three calculations have been performed in contoured nozzle no. 2 (whose length is 3.42 m and throat radius 0.005 m). The conditions correspond to test case no. 1[33]: $P_0 = 430$ bar for the total pressure and $H_0/RT_0 = 260$ for the reduced enthalpy. A quasi-one-dimensional approach has been used to save CPU time. Seven orders of magnitude for the decrease of quadratic residuals have been obtained.

The first calculation considers only the five chemical species (N_2, O_2, NO, N, and O) of the usual system with the *V–T* molecule–molecule and molecule–atom couplings (cf., Sec. III.A). The two others include H_2O with V–T couplings (cf. Sec. IV.C). For each molecule N_2 or O_2 colliding with H_2O, we have selected a low reaction rate and a rapid reaction rate.

The first model consists of the low reaction rate for N_2–H_2O (Ref. 24) and O_2–H_2O (Ref. 16); the second model consists of the rapid reaction rate for N_2–H_2O (Ref. 22) and O_2–H_2O (Ref. 31). A mass fraction equal to 0.02 for H_2O has been assumed in the gas mixture.

1. Results

The results are shown in Figs. 4–7. Figure 4 presents the temperature distributions along the axis for the case without water. The N_2 vibrational temperature is about 1968 K at the nozzle exit, whereas the O_2 vibrational temperature is 606 K and the translational temperature is 422 K. In this calculation, the relaxation of N_2 and O_2 occurs through the V–T transfers with the molecules (N_2, O_2, and NO) and the atoms (N and O) of the gas mixture with relaxation rates given by Ref. 13 for the molecules and by Ref. 14 for the atoms.

Figure 5 shows the comparison of the N_2 vibrational temperature for the three calculations. The first model leads to a decrease equal to 40 K with respect to the case without water, whereas for the second model the decrease reaches 300 K.

The two models yield small differences in the O_2 vibrational temperature: an increase of 9 K with the first model and a decrease of 8 K with the second model. These variations correspond to the whole V–T coupling occurring in the mixture. The O_2 molecule was not far from equilibrium in the calculation without water, and so the effect of H_2O is less important than for N_2.

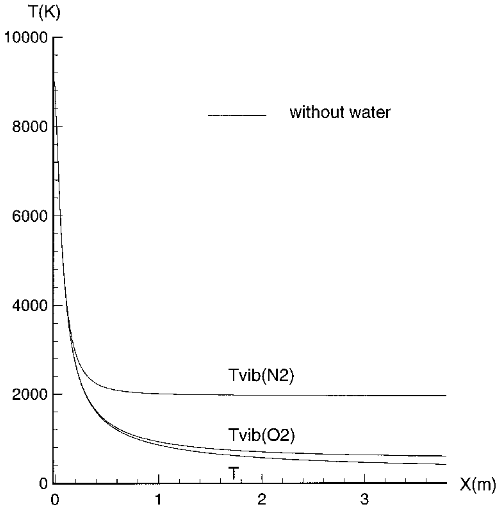

Fig. 4 Temperature distributions along the axis (F4).

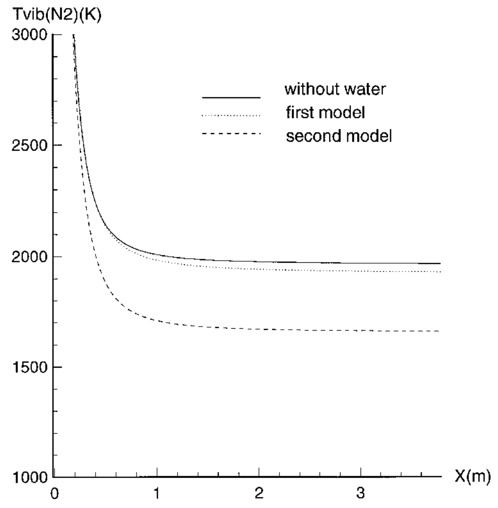

Fig. 5 Model comparisons for N_2 vibrational temperature (F4).

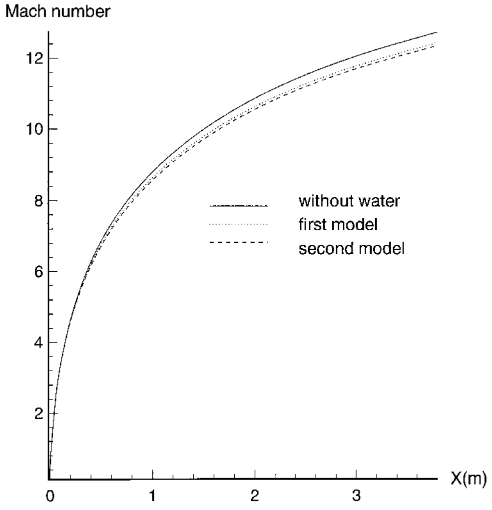

Fig. 6 Mach number distributions (F4).

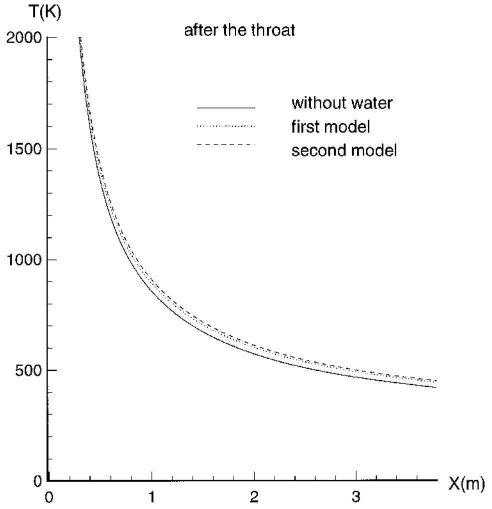

Fig. 7 Translational temperature distributions (F4).

The Mach number distributions are presented in Fig. 6. The second model gives a decrease in Mach number of about 0.4, corresponding to an increase of 30 K in the static temperature, shown in Fig. 7.

B. LBK Wind Tunnel

Another application deals with the hypersonic flow in the LBK wind tunnel of DLR. Experimental results are available in this case. The total length, the throat diameter, and the half angle of this nozzle are, respectively, equal to 0.4 m, 0.029 m, and 12 deg. The conditions are the experimental ones: $p_0 = 1.29 \times 10^5$ Pa and $T_0 = 3748$ K. The measurements have been carried out at a position 0.555-m downstream of the nozzle exit. The experimental setup and the CARS theory are described.[2,3] Three calculations have also been performed in this case. A first calculation does not consider water. A second calculation corresponds to the second model previously described. A third calculation includes, in addition to the second model, the V–V O_2–H_2O process (third model). A mass fraction equal to 0.02 for H_2O is assumed.

1. Results

The results are presented in Figs. 8–11. Figure 8 represents the temperature distributions along the axis calculated without

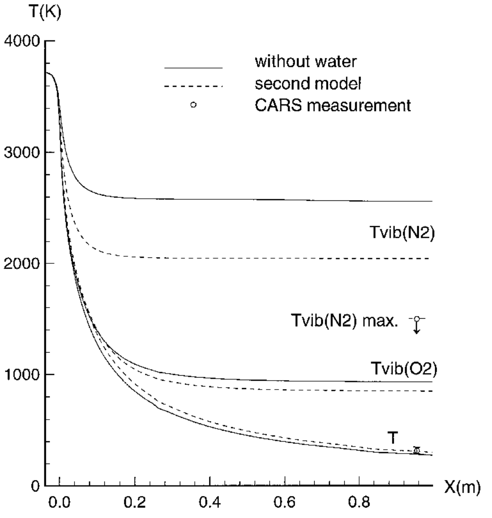

Fig. 8 Temperature distributions along the axis (LBK).

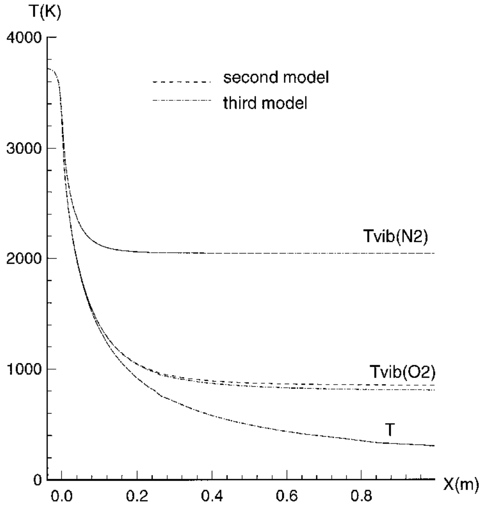

Fig. 9 Temperature distributions along the axis (LBK).

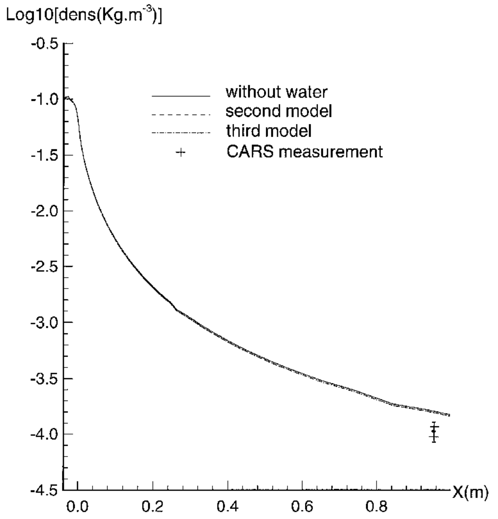

Fig. 10 Total density distributions along the axis (LBK).

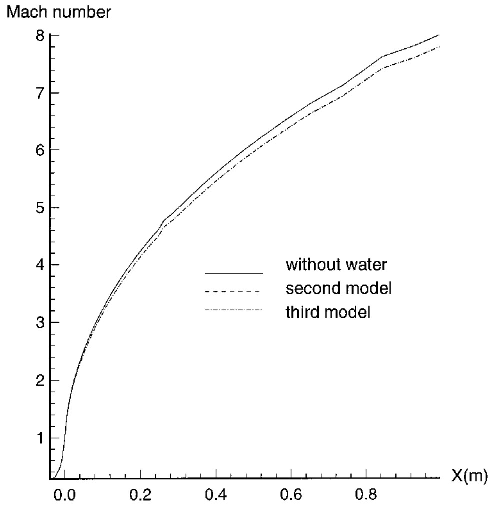

Fig. 11 Mach number distributions along the axis (LBK).

water and for the second model. An important decrease equal to 500 K is observed on the vibrational temperature of N_2 at the location of the measurements, whereas it is about 80 K for O_2. Figure 8 also shows the experimental points: neglecting the rotational lines below $J = 6$ in the Boltzmann diagram, the rotational distribution might be approximated by a straight line with a corresponding temperature $T_{\rm rot}^{\rm CARS} = 320\ {\rm K} \pm 10\ {\rm K}$. Assuming that $T_{\rm trans} = T_{\rm rot}$, the experimental point is plotted in Fig. 8 (the error bar is small according to the scale of this figure). Good agreement between experiment and calculations is found with the results given with the second model $T_{\rm trans}^{\rm calc} = 310\ {\rm K}$ at the location of the experiment. For the case without water, the calculation gives $T_{\rm trans}^{\rm calc} = 285\ {\rm K}$.

Very weak signals were observed in the spectral region of the $v = 1$ vibrational band and no rotational structure was detected. Nevertheless, an upper and lower bound might be placed on the vibrational temperature from this result. The lower limit was 320 K, i.e., by assuming that the gas in the freestream was in thermodynamic equilibrium. The upper limit was estimated by calculating theoretical spectra with different vibrational temperatures until the vibrational band appeared above the experimental background level. A temperature of 1500 K was then found. Above this temperature, the vibrational $v = 1$ band would have been observed experimentally. However, the calculated vibrational nitrogen temperature is too large in the two calculations (Fig. 8), although the faster relaxation rate (second model) has been chosen. These results imply that the mass fraction of H_2O may have been more important than 0.02 in the flow. However, no attempt to reproduce the value of 1500 K has been tried by changing the water mass fraction in the calculation because the measured N_2 vibrational temperature is too uncertain. Further experimental work is here needed. Another explanation is that other chemical species than those considered in the calculations cause N_2 to relax, or that some important reaction rates such as the one associated with the vibrational relaxation during N_2–O collisions are more effective than calculated.

Figure 9 shows a comparison of the results given by the second and the third models. The N_2 vibrational temperature does not change noticeably, whereas the O_2 vibrational temperature decrease is about 50 K, because of the V–V coupling.

Figure 10 shows the calculated total density distributions and the comparison with the experimental values. All of the calculations give about the same result. When the vibrational temperature is assumed to be 320 K, the measured total density is found to be $9.7 \pm 1.2 \times 10^{-5}\ {\rm kg/m^3}$. Assuming a vibrational temperature of 1500 K leads to a measured total density equal to $12.1 \pm 1.2 \times 10^{-5}\ {\rm kg/m^3}$. The agreement between calculations and experiment at the nozzle exit is rather good with this latter value.

At last, we see the Mach number distributions. A maximum variation equal to 0.2 is observed at a distance of 0.955 m from the throat between the case without water and the two models (second and third).

Conclusions

We have applied the CELHYO code to the simulation of the flow in two high-enthalpy wind tunnels. For this first study concerning contaminants, water has been considered. Its effect on the vibrational relaxation of N_2 and O_2 has been computed. Noticeable differences with and without water are found. However, the water mass fraction is not precisely known, which makes the comparison between computations and experiments difficult. We have thus completed a detailed study of the data provided for different relaxation processes of the two molecules (N_2 and O_2) and noticed that atoms are among the most effective vibrational catalysts of vibrational de-excitation. Then, to improve the chemistry models that apply for gas mixtures in wind tunnels, it is necessary to precisely determine (using experiments and calculations) the reaction rates that are associated with collisions between N_2 (or O_2) and the catalysts that may be present in the gaseous mixture (e.g., H_2O, Cu, O, . . .). The mass fractions of these catalysts also have to be precisely known. All of these determinations may be particularly difficult, but the clarification of many unexplained experimental results depends on such an analysis. The problems caused by copper may soon be alleviated by the use of carbon parts instead of copper parts in the F4 wind-tunnel chamber (particularly for the electrodes). We thus expect to simulate more accurately hyperenthalpic flows in wind tunnels.

Acknowledgment

This work was partially supported by a European Space Agency contract.

References

[1] Vérant, J. L., and Sagnier, P., "Assessment of Total Conditions and Flow Thermochemical Nature in the ONERA F4 High Enthalpy Wind Tunnel," AIAA Paper 96-2239, June 1996.

[2] Grisch, F., Bouchardy, P., and Péalat, M., "CARS Studies in Hypersonic Flows," AIAA Paper 93-3047, July 1993.

[3] Massabieaux, B., Gousset, G., Lefebvre, M., and Péalat, M., "Determination of $N_2(X)$ Vibrational Level Populations and Rotational Temperatures Using CARS in a D.C. Low Pressure Discharge," *Journal de Physique*, Vol. 48, 1939, 1987, pp. 1939–1949.

[4] Coquel, F., Flament, C., Joly, V., and Marmignon, C., "Viscous Nonequilibrium Flow Calculations," *Computing Hypersonic Flows*, edited by J. J. Bertin, J. Périaux, and J. Ballmann, Vol. 3, Birhäuser, Boston, 1993.

[5] Hurle, I. R., Russo, A. L., and Gordon, H. J., "Spectroscopic Studies of Vibrational Nonequilibrium in Supersonic Nozzle Flows," *Journal of Chemical Physics*, Vol. 40, No. 8, 1964, pp. 2076–2089.

[6] Fisher, E. R., and Smith, G. K., "Vibrational Relaxation by Metal Atoms," *Chemical Physics Letters*, Vol. 6, No. 5, 1970, pp. 438–440.

[7] Buchwald, M. I., and Wolga, G. J., "Vibrational Relaxation of $CO_2(001)$ by Atoms," *Journal of Chemical Physics*, Vol. 62, No. 7, 1975, pp. 2828–2832.

[8] Shin, H. K., "Self-Relaxation of Vibrationally Excited H_2O Molecules," *Journal of Chemical Physics*, Vol. 98, No. 3, 1993, pp. 1964–1978.

[9] Kurian, J., and Sreekanth, A. K., "Laser Schlieren Study of Vibrational Relaxation of N_2 by H_2O," *Chemical Physics*, Vol. 114, 1987, pp. 295–303.

[10] Anderson, J. D., Jr., "Time-Dependent Analysis of Population Inversions in an Expanding Gas," *Physics of Fluids*, Vol. 13, No. 8, 1970, pp. 1983–1989.

[11] Gardiner, W. C., Jr., *Combustion Chemistry*, Springer–Verlag, New York, 1984.

[12] Landau, L., and Teller, E., "Zur Theorie der Shalldispersion," *Physikalische Zeitschrift der Sowjetunion*, Vol. 10, 1936, pp. 34–43.

[13] Millikan, R. C., and White, D. R., "Systematics of Vibrational Relaxation," *Journal of Chemical Physics*, Vol. 39, No. 12, 1963, pp. 3209–3213.

[14] Thivet, F., Perrin, M. Y., and Candel, S., "A Unified Nonequilibrium Model for Hypersonic Flows," *Physics of Fluids A*, Vol. 3, 1991, pp. 2799–2812.

[15] Coquel, F., Joly, V., and Marmignon, C., "Méthodes de Decentrement Hybrides pour la Simulation d'Ecoulements en Déséquilibre Thermique et Chimique," Progress and Challenges in CFD Methods and Algorithms, 77th AGARD FDP Symposium, Seville, Spain, Oct. 1995, pp. 34.1–34.11.

[16] Taylor, R. L., "Energy Transfer Processes in the Stratosphere," *Canadian Journal of Chemistry*, Vol. 52, 1974, pp. 1436–1451.

[17] Tuesday, C. S., and Boudart, M., Princeton Univ., Tech. Note 7, Contract AF 33(038)-23976, Princeton, NJ, Jan. 1955.

[18] Finzi, J., Hovis, F. E., Panfilov, V. N., Hess, P., and Moore, C. B., "Vibrational Relaxation of Water Vapor," *Journal of Chemical Physics*, Vol. 67, No. 9, 1977, pp. 4053–4061.

[19] Kung, R. T. V., and Center, R. E., "High Temperature Vibrational Relaxation of H_2O by H_2O, He, Ar, and N_2," *Journal of Chemical Physics*, Vol. 62, No. 6, 1975, pp. 2187–2194.

[20] Shin, H. K., "Vibrational Relaxation of Water Molecules Near Room Temperature," *Journal of Chemical Physics*, Vol. 69, No. 3, 1978, pp. 1240–1245.

[21] Zuckerwar, A. J., and Meredith, R. W., "Acoustical Measurements of Vibrational Relaxation in Moist N_2 at Elevated Temperatures," *Journal of the Acoustical Society of America*, Vol. 71, No. 1, 1982, pp. 67–73.

[22] Taylor, R. L., and Bitterman, S., "Survey of Vibrational Relaxation Data for Processes Important in the CO_2-N_2 Laser System," *Reviews of Modern Physics*, Vol. 41, No. 1, 1969, pp. 26–47.

[23] Rosenberg, Von, C. W., Jr., Bray, K. N. C., and Pratt, N. H., "Shock Tube Vibrational Relaxation Measurements: N_2 Relaxation by H_2O and the CO-N_2 V-V Rate," *Journal of Chemical Physics*, Vol. 56, No. 7, 1972, pp. 3230–3237.

[24] Center, R. E., and Newton, J. F., "Vibrational Relaxation of N_2 by H_2O," *Journal of Chemical Physics*, Vol. 68, No. 8, 1978, pp. 3327–3333.

[25] Rapp, D., and Englander-Golden, P., "Resonant and Near-Resonant Vibrational-Vibrational Energy Transfer Between Molecules in Collisions," *Journal of Chemical Physics*, Vol. 40, 1964, pp. 573–575.

[26] Moore, C. B., "Vibration-Rotation Energy Transfer," *Journal of Chemical Physics*, Vol. 43, 1965, pp. 2979–2986.

[27] Nagel, J., and Rogovin, D., "Vibrational Deactivation of Nitrogen by Water Vapor," *Proceedings of the International Conference on Lasers*, Science Applications, Inc., La Jolla, CA, 1979, pp. 610–616.

[28] Schwartz, R. N., Slawsky, Z. I., and Herzfeld, K. F., "Calculation of Relaxation Times in Gases," *Journal of Chemical Physics*, Vol. 20, No. 10, 1952, pp. 1591–1599.

[29] Bass, H. E., Keeton, R. G., and Williams, D., "Vibrational and Rotational Relaxation in Mixtures of Water Vapor and Oxygen," *Journal of the Acoustical Society of America*, Vol. 60, No. 1, 1976, pp. 74–77.

[30] Blauer, J. A., and Nickerson, G. R., "A Survey of Vibrational Relaxation Rate Data for Processes Important to CO_2—N_2—H_2O Infrared Plume Radiation," AIAA Paper 74-536, June 1974.

[31] Nickerson, G. R., "Nonequilibrium Radiation Model for Exhaust Plumes," Air Force Rocket Propulsion Lab., TR-74-74, March 1975.

[32] Lang, V. I., "Relaxation Processes of Vibrationally Excited H_2O in the Mesosphere and Thermosphere," The Aerospace Corp., TOR-0091(6078)-2, Los Angeles, CA, Sept. 1991.

[33] *Proceedings of the 4th European High Velocity Database Workshop*, ESTEC, Noordwijk, The Netherlands, 1996 (to be published).